FIELD TRIP GUIDE: A PROFILE FROM MIGMATITES TO SPODUMENE PEGMATITES (STYRIA, AUSTRIA)

7th April 2019
St. Radegund

Berichte der Geologischen Bundesanstalt, 134

Geological Survey of Austria

Field trip guide: A profile from migmatites to spodumene pegmatites (Styria, Austria)

7th April 2019

St. Radegund, Austria

RALF SCHUSTER, TANJA KNOLL, HEINRICH MALI,
BENJAMIN HUET & GERIT E.U. GRIESMEIER

Bundesministerium
Bildung, Wissenschaft
und Forschung

Geologische Bundesanstalt

Berichte der Geologischen Bundesanstalt, 134
ISSN 1017-8880

Field trip guide: A profile from migmatites to spodumene pegmatites (Styria, Austria)

Ralf Schuster, Tanja Knoll, Heinrich Mali, Benjamin Huet & Gerit E.U. Griesmeier

Ralf Schuster, Tanja Knoll, Benjamin Huet & Gerit E.U. Griesmeier: Geologische Bundesanstalt, Neulinggasse 38, 1030 Vienna, Austria.

Heinrich Mali: Montanuniversität Leoben, Department Applied Geosciences and Geophysics, Peter-Tunner-Straße 5, 8700 Leoben

Recommended citation / Zitiervorschlag

Schuster, R., Knoll, T., Mali, H., Huet, B. & Griesmeier, G.E.U. (2019): Field trip guide: A profile from migmatites to spodumene pegmatites (Styria, Austria). – Berichte der Geologischen Bundesanstalt, 134, 29 p., Vienna.

Cover design: Monika Brüggemann-Ledolter (Geologische Bundesanstalt).
Cover pictures: Spodumene pegmatite at Garrach (Styria, Austria) (upper picture: Christine Hörfarter, lower picture: Ralf Schuster)

Wien, November 2019

Alle Rechte für das In- und Ausland vorbehalten.

© Geologische Bundesanstalt, Wien
Technische Redaktion: Christoph Janda

Medieninhaber, Herausgeber und Verleger:
Geologische Bundesanstalt, Wien
Neulinggasse 38, 1030 Wien
www.geologie.ac.at

Druck: Riegelnik Ges.m.b.H, Piaristengasse 17–19, 1080 Wien

Ziel der „Berichte der Geologischen Bundesanstalt“ ist die Verbreitung wissenschaftlicher Ergebnisse durch die Geologische Bundesanstalt. Die „Berichte der Geologischen Bundesanstalt“ sind im Handel nicht erhältlich.

Preface

Rare element pegmatite is an important host for critical elements crucial to the high-tech industry (Li, Nb, Ta …). All types are traditionally interpreted as products of highly fractionated granitic melts and thought to be genetically linked to large parental fertile granite bodies. Recent studies, however, suggest that some pegmatite fields including rare element pegmatite could have an anatectic origin. Since 2015, a series of joint projects lead by the Geological Survey of Austria (GBA) and the Montanuniversität Leoben (MUL) targeted spodumene ($LiAlSi_2O_6$) pegmatite occurrences within the Austroalpine Unit of the Eastern Alps. The results argue that the studied rare element pegmatite have an anatectic origin.

To present the spodumene pegmatite of the Austroalpine Unit and its field relation to its hostrocks, a one-day field trip to the St. Radegund area (Styria, Austria) was offered at the European Geosciences Union (EGU) 2019 conference in the frame of the session “Impacts of partial melting on the evolution of the continental crust: different views, one topic”. About 40 participants from ten countries visited key outcrops providing an exceptional insight into the genetic relationships between migmatite, simple pegmatite, leucogranite and spodumene pegmatite. Field observations were discussed in the light of geochemical and geochronological data acquired on the visited outcrops and the surrounding area.

We published this field trip guide to provide a basis for future excursions.

Content

1. Introduction

In the Austroalpine Unit of the Eastern Alps, spodumene pegmatites spread heterogeneously across an E–W distance of more than 400 km (Fig. 1). These pegmatites are classified as albite-spodumene pegmatites of the rare element (RE) class (GÖD, 1989; ČERNÝ & ERCIT, 2005). They are always spatially associated with simple pegmatite and leucogranite bodies lacking remarkable RE-mineralizations. Simple pegmatite and leucogranite bodies are considered to be the products of anatexis (STÖCKERT, 1987; THÖNI & MILLER, 2000) and formed during the Permian event, which is characterized by lithospheric extension, causing crustal basaltic underplating, high temperature-low pressure (HT/LP) metamorphism and intense magmatic activity within the crust (SCHUSTER & STÜWE, 2008). In a recent study (ILICKOVIC et al., 2017; KNOLL et al., 2018; MALI et al., 2019; SCHUSTER et al., 2017), the genetic relationship of spodumene pegmatite with respect to simple pegmatite and leucogranite was worked out, based on field relations, Rb-Sr and Sm-Nd geochronology, bulk-rock geochemistry and mineral Laser Ablation-ICPMS analyses. The results indicate a formation of all of these magmatic rocks from anatectic melts generated during prograde HT/LP metamorphism of specific Al-rich metapelites and following fractionated crystallization of simple pegmatite, leucogranite, moderate fractionated pegmatite and spodumene pegmatite. Additionally, a quantitative model explaining the Li-transfer from metapelite into spodumene pegmatite was proposed (SCHUSTER et al., 2019; KNOLL et al., in prep.).

In the course of the excursion to the St. Radegund area (Styria/Austria), the field relations of the above-mentioned rocks are presented within a single nappe of the Austroalpine Unit. At the base of the Radegund Nappe, migmatic micaschist and paragneiss with aborted melt formation occur, whereas the top consists of staurolite-bearing micaschist with spodumene pegmatite bodies therein. This allows to study an upright section through the Permian middle crust, in spite of a pressure dominated amphibolite facies overprint and related deformation, which occurred during the Eoalpine event in the Cretaceous.

This field guide includes a short introduction to the regional geology of the Eastern Alps, some remarks on the route from Vienna to the St. Radegund area and a detailed description of the field stops.

2. Geological overview of the Eastern Alps

The Alpine orogen developed from two continental and two oceanic realms existing in Late Jurassic to Cretaceous times (Fig. 1). Additionally, the lowermost tectonic units represented by the Allochthonous Molasse in the Eastern Alps, formed from parts of the northern foreland basin during post-Oligocene shortening. The former European continental margin was incooperated since the Eocene and comprises the Helvetic nappes appearing along the northern front and the Subpenninic nappes present in the more internal part of the orogenic belt. The overlying Penninic nappes are derived from the Penninic Ocean (Alpine Tethys) and continental fragments therein. Together with the Subpenninic nappes, they experienced Alpine tectonics and metamorphism, mainly in the Eocene to Miocene. The Austroalpine and the Southalpine Unit, separated by the Periadriatic fault, are both derived from the Adriatic Microcontinent and now occur on top of the previously described units. The Austroalpine nappes were sheared off during the Eoalpine event in the Cretaceous and the individual nappes experienced variegated tectonic and metamorphic overprints during subduction, nappe stacking and exhumation. All the above-mentioned units represent the northwest-verging pro-

wedge of the Alpine orogen, whereas the Southalpine Unit formed as a south-verging retro-wedge mainly after the Oligocene. Tectonic slices derived from the Neotethys Ocean, referred to as the Meliata Unit, occur within the Austroalpine nappe pile. They were mobilized in the Jurassic and reached their present position by out-of-sequence thrusting in the Early Cretaceous (FROITZHEIM et al., 2008).

While Permian magmatic rocks occur in all major tectonic units composed of continental crust, Permian pegmatites are restricted to those derived from the Adriatic Microcontinent. The continental crust of this domain was affected by intense magmatism during a Cambro-Ordovician event related to extension at the northern margin of Gondwana, the late Devonian to Carboniferous Variscan collisional event in the course of Pangea formation, a Permian extensional event within Pangea and finally the Alpine collisional event since the earliest Cretaceous. As pegmatite formation occurred during the Permian extensional event and they were overprinted during the Alpine event, these two events are described in more detail.

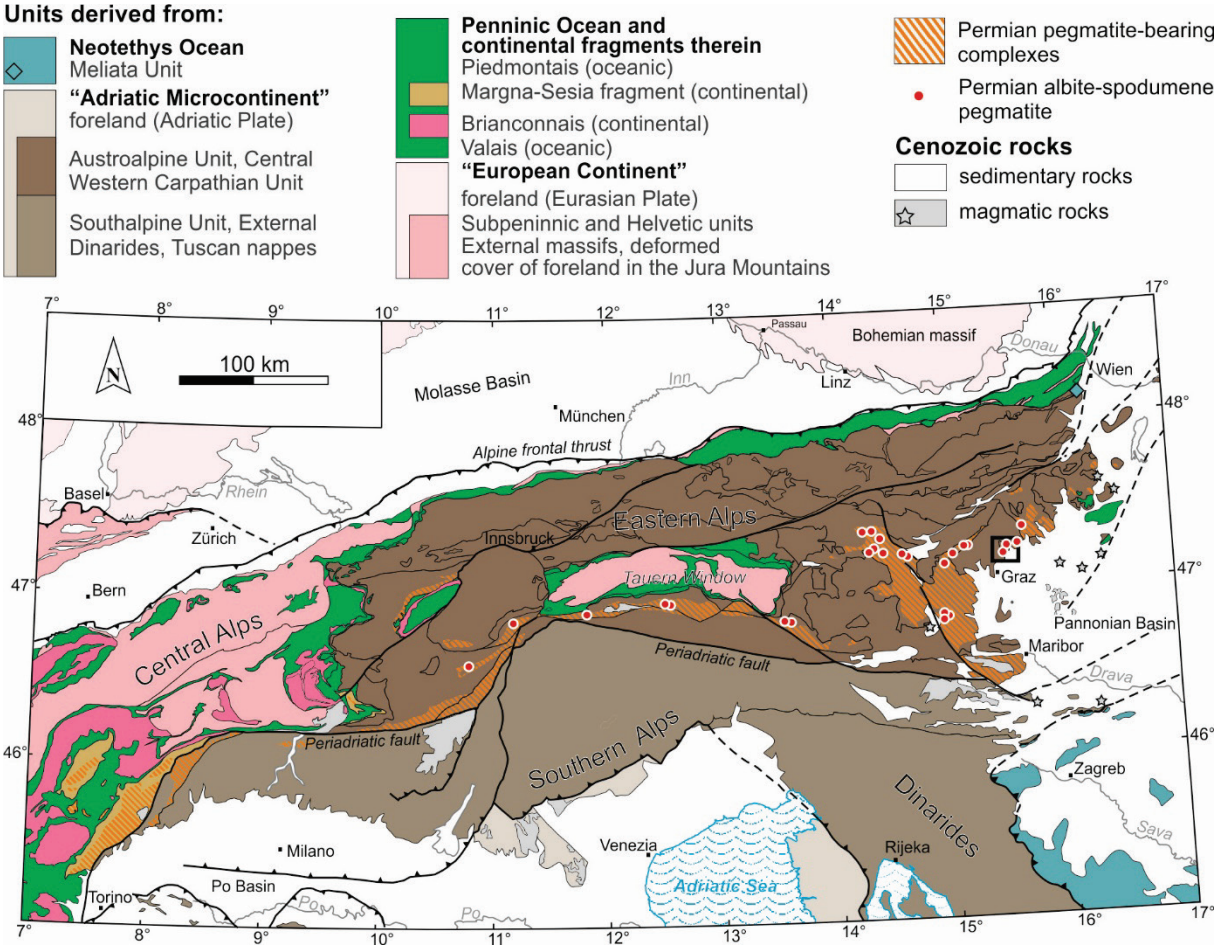

Fig. 1: *Tectonic map of the Alps showing the paleogeographic origin of the major tectonic units of the Alps (modified after FROITZHEIM et al., 2008). Additionally, the distribution of complexes containing Permian pegmatite and spodumene pegmatite is highlighted (modified after MALI, 2004 and KNOLL et al., 2018). Black square indicates the area of St. Radegund shown in Figure 6.*

2.1. Permian extensional event

The Permian event in the Alps followed in the wake of the Variscan tectonic evolution. Lithospheric extension affected the Adria derived Austroalpine and Southalpine Unit, but also the Europe derived Brianconnais and Subpenninic Unit. The Permian event onset at about 290 Ma may be considered when crustal thickness decreased below normal and thus cannot be related to gravitational collapse of the Variscan orogen anymore. Basaltic melts rose up from the mantle to the base of the crust and caused intense magmatic activity and related HT/LP metamorphism. Peak metamorphic conditions were reached at about 280–260 Ma at a geothermal gradient of up to 45° C/km (HABLER & THÖNI, 2001; SCHUSTER et al., 2001; KUNZ et al., 2018). Subsequently, the metamorphosed rocks were not exhumed, but the lithosphere cooled down slowly to a steady state geotherm of c. 25° C/km at about 200 Ma. Slow cooling of the lithosphere caused continuous subsidence in late Permian and throughout Triassic time. This subsidence triggered the deposition of more than 3 km thick Permian clastic successions and Triassic carbonate platform sediments (SCHUSTER & STÜWE, 2008).

A map showing the distribution of the Permian metamorphic grade and related magmatic and sedimentary rocks is given in Figure 2. Numbers in the text refer to key areas indicated also therein. A section through the base of the Permian crust with gabbroic and dioritic intrusions

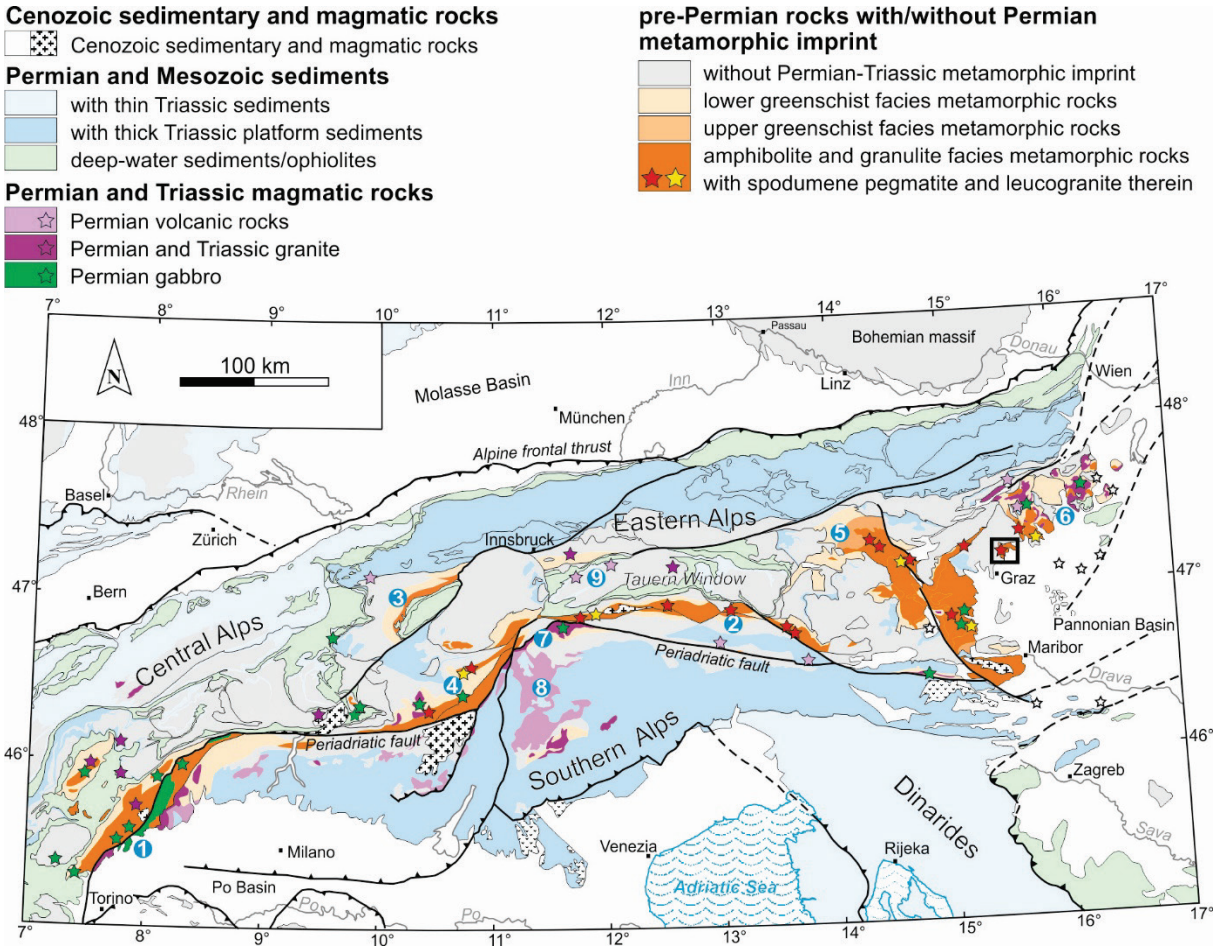

Fig. 2: *Map of the Alps showing the distribution of Permian metamorphism and related magmatic and sedimentary rocks. Pegmatite bodies are frequent in most of the amphibolite to granulite facies units. Numbers refer to the text and the black square indicates the area of St. Radegund shown in Figure 6. Map modified from SCHUSTER & STÜWE (2008).*

as well as restitic kinzigites is exposed in the Ivrea Zone (QUICK et al., 1995) (1). Deep crustal levels are indicated by amphibolite to granulite facies rocks with sillimanite, andalusite and indications of anataxis (KUNZ et al., 2018). Therein, gabbro, diorite and granite bodies as well as pegmatite dikes occur. Such sections are well preserved in the Kreuzeck-Gailtaler Alpen Nappe (2), at the base of the Silvretta Nappe (3) or within the Campo Nappe (4) (SCHUSTER et al., 2001; THÖNI, et al., 2008). From the Permian middle crust upper greenschist facies metamorphic units with garnet-bearing assemblages are known e.g. from the Donnersbach Nappe (5). Somewhat higher levels are characterized by large bodies of biotite-granite, which intruded within greenschist facies metapelite partly showing contact phenomena. Such kind of basement can be studied in the easternmost part of the Eastern Alps (6), but also in the Southalpine Unit (7). Within the uppermost crust, subvolcanic dikes and intrusions occur and at the surface Permian grabens are filled with sedimentary piles typically containing volcanic layers (CASSINIS et al., 2012). The most famous volcanic centre is represented by the Bozen quartzporphyry (8), but similar rocks are also known from the Subpenninic nappes of the Tauern Window (9).

Fieldwork and detailed mapping revealed that Permian pegmatite and leucogranite in the Eastern Alps are restricted to distinct complexes with typical lithological associations and petrological features (KNOLL et al., 2018). These complexes stayed in lower to middle crustal levels during the Permian. Three different domains can be distinguished (Fig. 3).

(1) In structurally lower parts, pegmatitic patches, narrow pegmatite dikes and larger feldspar dominated pegmatite dikes occur in aluminosilicate-bearing, garnet-rich micaschist and paragneiss representing restites of initial anatexis. The pegmatitic patches have a thickness of a few centimeters to decimeters. Associated pegmatite formed by accumulation of melts from the patches is present as networks of centimeter thick veins or up to a few meters thick dikes. They are concordant and mostly composed of feldspar and quartz. According to data from surrounding micaschist and paragneiss this level stayed in a depth of c. 20 km and experienced upper amphibolite to granulite facies metamorphic conditions (~0.65 GPa and 650° C; KNOLL et al., in prep.) during the Permian event. (2) Structurally higher domains are characterized by frequent concordant, simple pegmatites of several meters thickness and mineral assemblages with feldspar, quartz, muscovite, garnet and tourmaline. In some places (e.g. Martell valley, Uttenheim valley, Geißrücken near Judenburg), associated inhomogeneous leucogranite bodies with pegmatitic and aplitic striae occur. They extend up to a few kilometers in size. (3) Moderate fractionated pegmatite is present as partly discordant dikes in structurally uppermost levels. Feldspar, quartz, muscovite, garnet and tourmaline form the common assemblage, but additionally spodumene and beryl may be present. Very rarely, tiny grains of cassiterite, columbite and REE-minerals have been found. Spodumene pegmatite occurs in about a dozen places forming up to a few meters thick dikes with lengths up to more than one kilometer (GÖD, 1989; MALI, 2004; KNOLL et al., 2018), but they also occur as several decimeter sized boudins. The occurrence of contemporaneously formed garnet in surrounding micaschist and paragneiss, these pegmatite dikes intruded in upper greenschist facies conditions (~0.45 GPa at 500° C) at crustal levels of c. 17 km depth.

Muscovites from simple pegmatite, leucogranite, moderate fractionated pegmatite and spodumene pegmatite plot on continuous fractionation trends in the diagrams by ČERNÝ & ERCIT (2005). This trend is particularly notable for muscovite on the K/Rb versus Li and K/Rb versus Tl diagrams of Figure 4. The analyses show that the K/Rb ratio of muscovite progressively decreases from migmatite (254 to 337), simple pegmatite (27 to 448), leucogranite (22 to 193), moderate fractionated pegmatite (22 to 364) to spodumene pegmatite

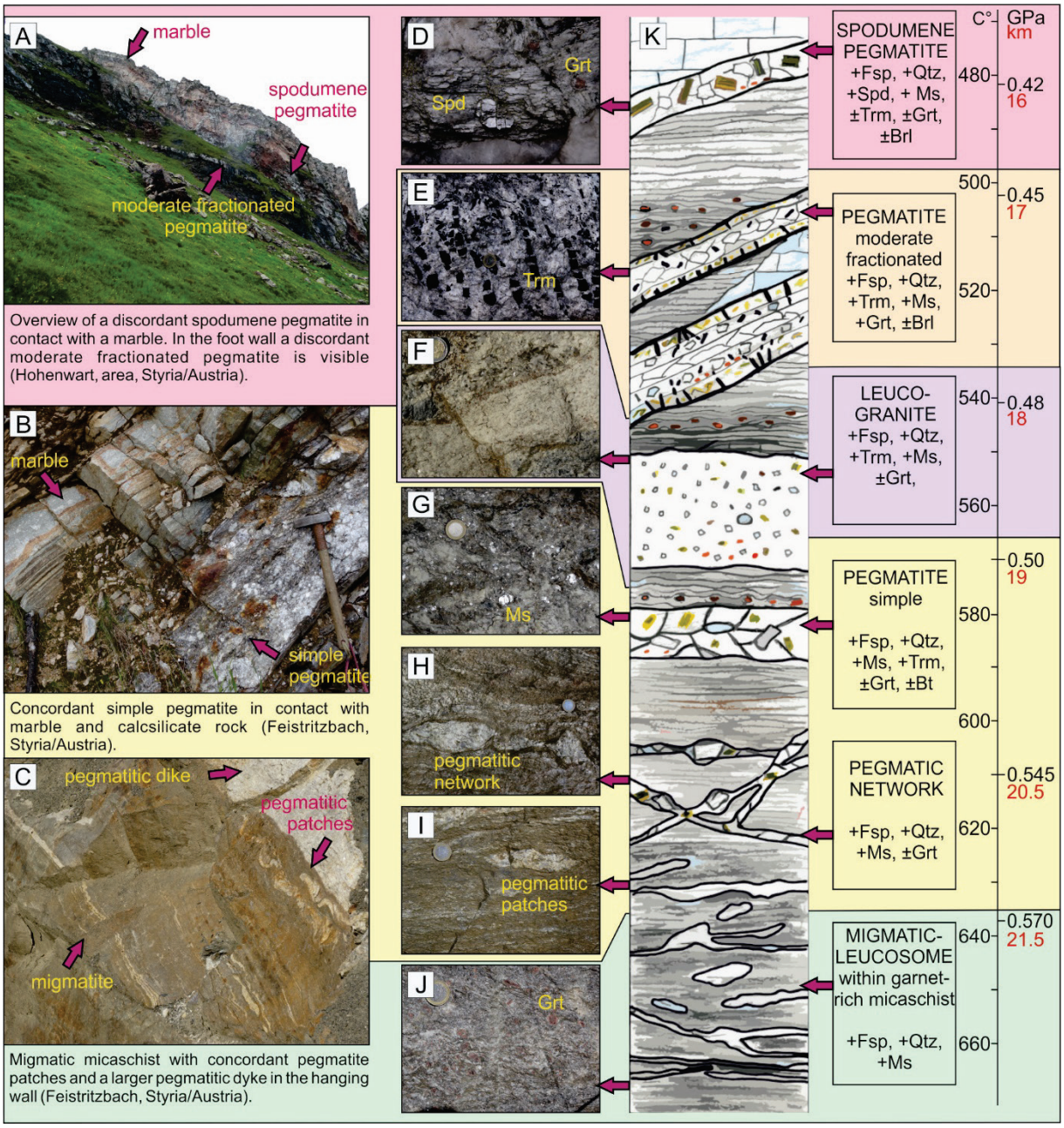

Fig. 3: *Synoptic diagram showing field relations for Permain pegmatites and leucogranites in the Austroalpine Unit of the Eastern Alps. As mentioned in the text a lower migmatic domain (green and yellow), a domain with evolved pegmatite and leucogranite (yellow and violet) and an upper domain with evolved pegmatite and spodumene pegmatite (orange and red) can be distinguished. Outcrop pictures of A) spodumene pegmatite, B) concordant simple pegmatite and C) migmatic micaschist with pegmatitic networks and dikes. Compilation of typical lithologies: D) spodumene pegmatite (width of image 7 cm), E) comb structures of deformed tourmaline (width of image 37 cm), F) inhomogeneous leucogranite (width of image 20 cm), G) muscovite pegmatite (width of image 25 cm), H) deformed pegmatitic network (width of image 40 cm), I) pegmatitic patches within deformed migmatic micaschist (width of image 30 cm), J) garnet-rich restitic paragneiss (width of image 20 cm). K) Schematic column shows the distribution of typical lithologies, magmatic assemblages and depth-pressure-temperature relations.*

Abbreviations: Spd = spodumene, Brl = beryl, Trm = tourmaline, Grt = garnet, Ms = muscovite, Fsp = alkali feldspar and plagioclase, Qtz = quartz.

(15 to 151). Additionally, the K/Rb ratio shows a negative correlation with the Li concentration (77–217 ppm in migmatite, 10–99 ppm in simple pegmatite, 36–785 ppm in leucogranite, 100–760 ppm in moderate fractionated pegmatite and 361–1,780 ppm in spodumene pegmatite, Figure 4A) as well as with the Tl concentration (1–3 ppm in migmatite, 1–19 ppm in simple pegmatite, 2–19 ppm in leucogranite, 1–19 ppm in moderate fractionated pegmatite and 2–28 ppm in albite-spodumene pegmatite, Figure 4B).

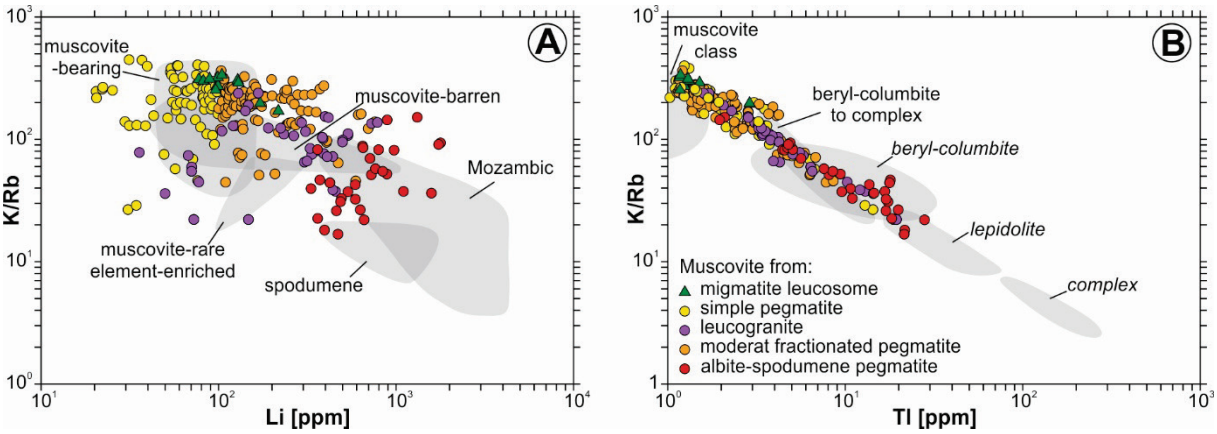

Fig. 4: *Trace element composition of muscovite from migmatite leucosome, simple pegmatite, moderate fractionated pegmatite, leucogranite and spodumene pegmatite. A) K/Rb ratio vs. Li. B) K/Rb ratio vs. Tl. The grey backgrounds refer to pegmatite groups defined in ČERNÝ & BURT (1984).*

2.2. Alpine collisional event

The Alpine collisional event is a consequence of the convergence between the African, Adriatic and Eurasian plates. Even though there is a general consensus about the paleogeographic framework, models with one or up to four suture zones have been proposed to explain the present day tectonic situation (Fig. 5) (e.g. FROITZHEIM et al., 1996; NEUBAUER et al., 2000; KURZ & FRITZ, 2003; JANÁK et al., 2015).

Following STÜWE & SCHUSTER (2010) collision initiated at an south(east) dipping intracontinental subduction zone within the Adriatic Microcontinent. The Austroalpine nappes formed during the consumption of the Adriatic continental crust from earliest Cretaceous until middle Late Cretaceous time (Eoalpine event). Some stayed at high crustal levels, whereas others were subducted and reached eclogite facies and even ultra-high pressure metamorphism. Peak conditions were reached at about 92 Ma in the early Late Cretaceous (THÖNI, 2006) followed by a medium pressure overprint during exhumation of the high-pressure rocks. In the eastern part of the Eastern Alps exhumation of the deeply buried units occurred by N- or NW-directed thrusting and S- to SE-directed extensional tectonics, causing the formation of a metamorphic extrusion wedge. The latter shows a lower part with an inverted metamorphic field gradient and an upper part with an upright metamorphic field gradient. Cooling ages are in the range of 90 to 70 Ma (HOINKES et al., 1999; THÖNI, 1999).

Ongoing subduction of the lithospheric plate caused the entrance of the Penninic oceanic domain into the subduction zone at about 85 Ma. Parts of the sediments, oceanic crust and uppermost mantle were sheared off and incorporated into the orogenic wedge referred to as Penninic nappes. After the closure of the ocean, European continental lithosphere got into the subduction zone in the Eocene at about 45 Ma (SCHMID et al., 2013). These processes referred

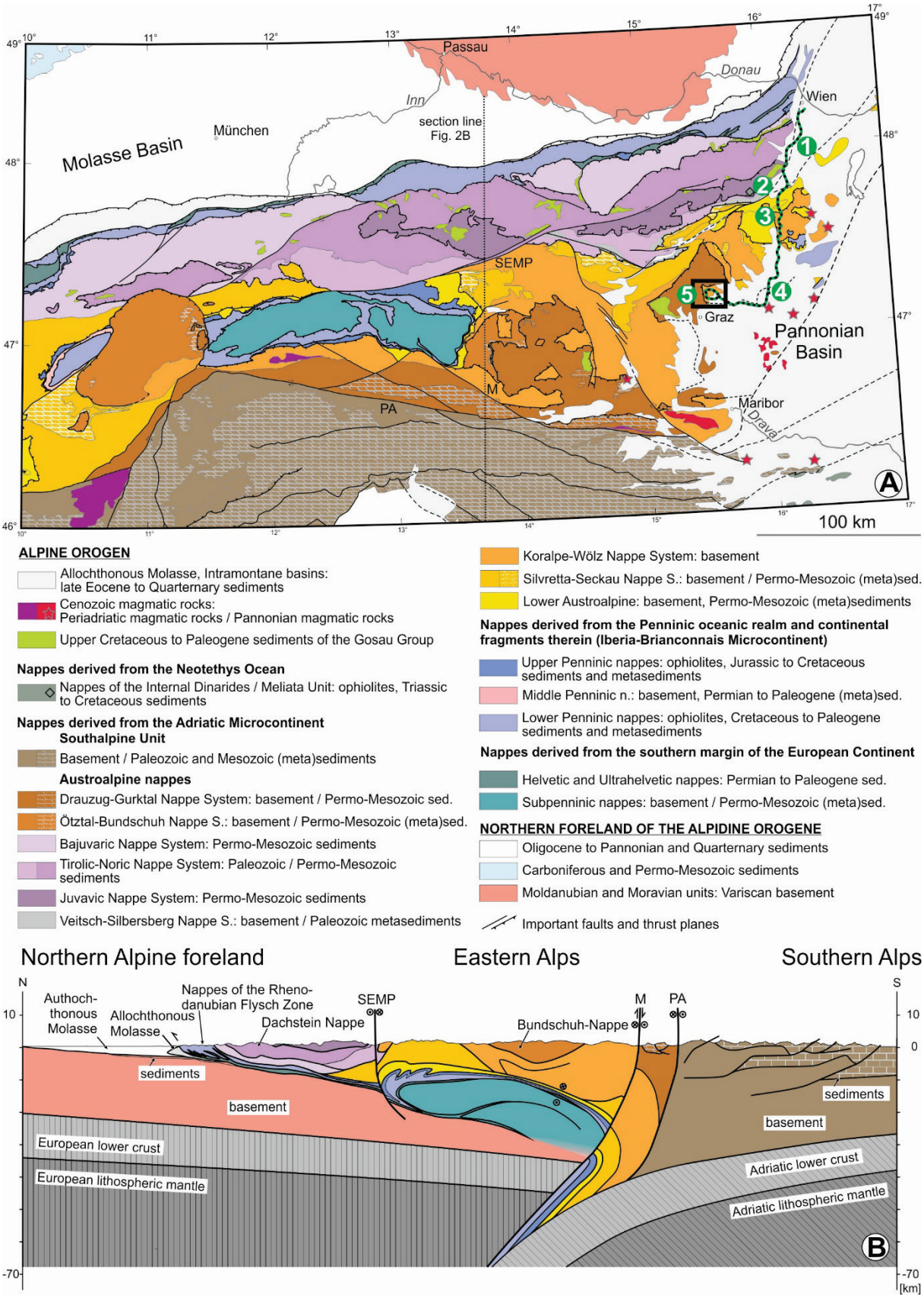

Fig. 5: *Tectonic map A) and section B) of the Eastern Alps according to the nomenclature in* FROITZHEIM *et al. (2008). SEMP = Salzach-Ennstal-Mariazell-Puchberg fault, M = Mölltal fault, PA = Periadriatic fault. The black square indicates the area of St. Radegund shown in Figure 6. Numbers refer to certain sections of the travelling route: 1 = Vienna Basin, 2 = Mt. Schneeberg area, 3 = Mt. Wechsel area, 4 = Styrian Basin (near Hartberg), 5 = Mt. Schöckl near to Graz.*

to as the Mesoalpine and Neoalpine events are dominating in the Central and Western Alps. They resulted in the formation of the Subpenninic and Helvetic nappes. In the Eastern Alps, the Neoalpine event caused a LT/HP metamorphism in the Penninic and Subpenninic nappes at 35–40 Ma (THÖNI, 1999). A subsequent medium pressure overprint at about 30–25 Ma is referred to as „Tauernkristallisation“ (SANDER, 1921; THÖNI, 1999). In Eocene to Oligocene times, the lithospheric slab formed since the Early Cretaceous teared below the Eastern Alps. Slab break-off induced uprise of hot asthenosphere and caused the Periadriatic magmatism (DAVIS & VON BLANKENBURG, 1995).

Indentation by the Adriatic microplate into the eastern part of the Alpine orogenic wedge since the beginning of the Miocene (23 Ma) caused further shortening of the northwest-vergent pro wedge. It reached about 50 % of the former width in the area of the western Tauern Window (SCHARF et al., 2013). Contemporaneous top-south-directed thrusting formed the retro wedge represented by the Southalpine Unit.

Also in the early Miocene, slab retreat in the course of the final closure of the Penninic Ocean in the Carpathian realm (FROITZHEIM et al., 2008) triggered thinning and eastward extrusion of the orogenic wedge. This process referred to as lateral extrusion (RATSCHBACHER et al., 1989) is responsible for the formation of a system of strike-slip and normal faults (GENSER & NEUBAUER, 1989; FÜGENSCHUH et al., 1997; SCHMID et al., 2013). Along these faults the Lower Engadine Window, Tauern Window and Rechnitz Window Group formed, exposing Penninic and Subpenninic units at the surface. Typical cooling ages for the rocks from within the tectonic windows are in the range of 25 to 15 Ma (DUNKL et al., 1998; LUTH & WILLINGSHOFER, 2008). Partly also the lowermost Austroalpine units (Lower Austroalpine nappes) adjacent to the windows experienced a structural and very-low to low grade Alpine metamorphic overprint (HOINKES et al., 1999; SCHUSTER et al., 2004). Major strike-slip faults are the Periadriatic, Inntal, Salzach-Ennstal-Mariazell-Puchberg, Mur-Mürz and Vienna Basin transfer faults. They have a major influence on the recent morphology, because fault bounded blocks like the Saualpe, Koralpe or Niedere Tauern mountain ranges were lifted up and tilted, whereas nearby basins like the Vienna, Styrian or Pannonian Basin developed. Thinning of the lithosphere and mantle upwelling below the Styrian Basin and Pannonian Basin caused synsedimentary magmatic activity (Pannonian magmatism). The occurrence of weak fault rocks triggered intense erosion along the faults, especially during the Quaternary glaciations.

3. Overview of the St. Radegund area

The area of interest around the village St. Radegund is shown in Figure 6 according to the geological map of FLÜGEL et al. (2011). In the northwestern part, nappes of the Austroalpine Unit form the surface, whereas in the southeast they are covered by transgressive sediments of the Neogene Styrian Basin. The Austroalpine Unit comprises nappes of the Koralpe-Wölz Nappe System in the footwall and the Drauzug-Gurktal Nappe System in a hanging wall position. The boundary in between is a moderately west dipping normal fault in the west and a steeply north dipping normal fault in the north.

Fig. 6: *Location of the field trip stops plotted on map sheet Graz (FLÜGEL et al., 2011) in the scale 1:50.000 from the Austrian Geological Survey. The analysed samples from staurolite-garnet-micaschist, migmatic micaschist, simple pegmatite, leucogranite, moderate fractionated pegmatite and spodumene pegmatite are plotted on the map. Dotted lines indicate traveling route.*

►

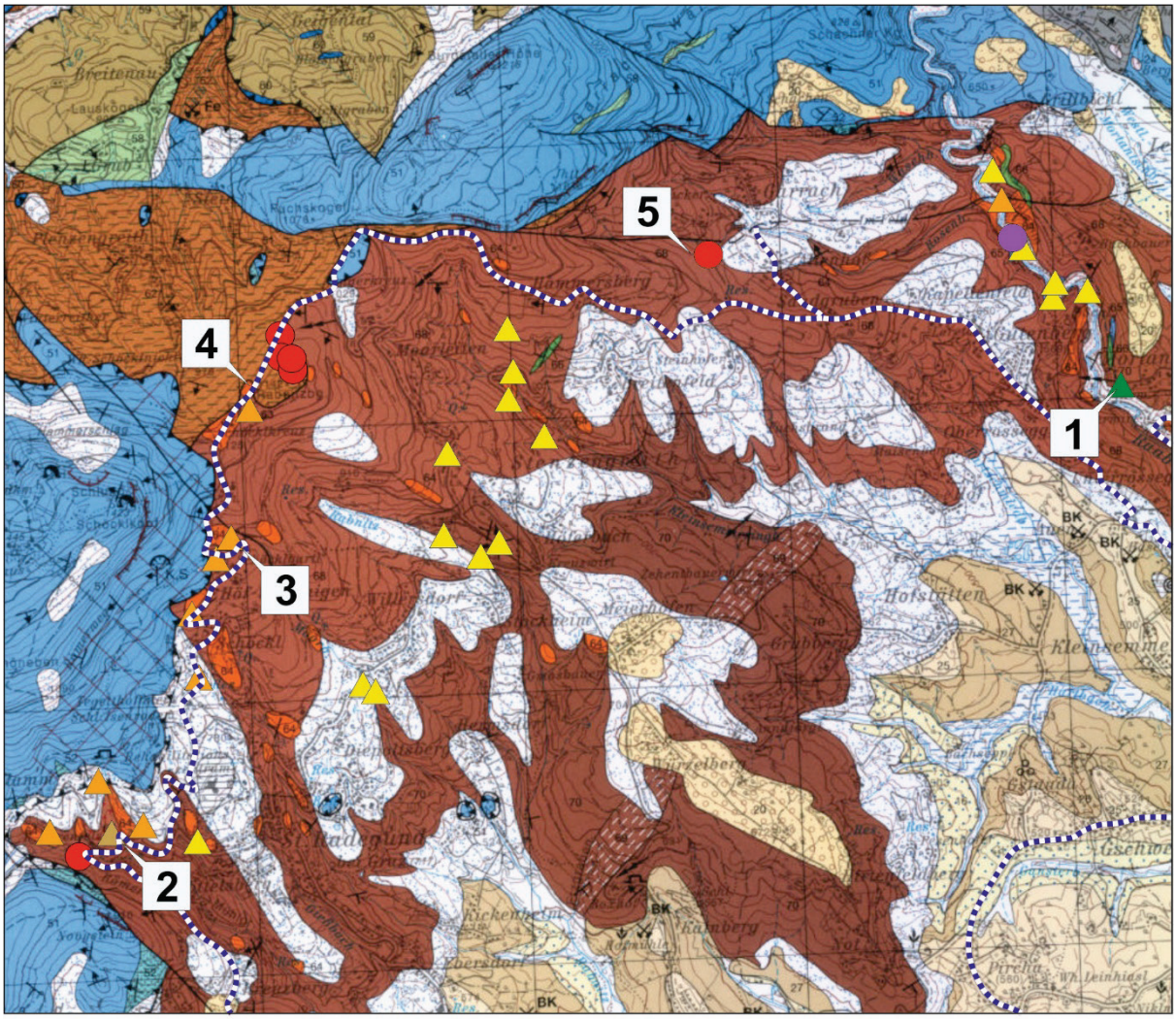

Quarternary deposites and features

- 1 Anthropogenic deposit
- 3 River and overbank sediment; silt, sand
- 4 Creek-bed sediment; gravel, sand, silt
- 6 Wetland
- 10 Talus; stones, gravel, sand
- 12 11 Scarp of mass movement and gravitational deposit; blocks
- 16 River sediment of floodplain terrace; gravel, sand, silt partly with loes cap (Würm/pre-Würm)

Styrian Basin (Neogene)

- 19 Peneplain (Pliocene)
- 23 Eggenberg Formation; reddish clay and carbonate breccia (early Miocene 17.5–13.5 Ma)
- 25 Ries Formation; gravel (Tortonium c. 10 Ma)
- Kleinsemmering Formation (Tortonium c. 10 Ma)
  - 26 silt, sand, marl, marly limestone
  - 27 silt, fine-sand, brown coal

Drauzug-Gurktal Nappe System

Schöckel Nappe

- 51 Schöckelkalk Formation; calcitic marble (Givetian?)
- 52 Raasberg Formation, dolomite, marble, quarzite (Pragian? – Givetian?)
- 53 dolomite, marble (Eifelian? – Givetian?)
- 54 quarzite, meta-conglomerate, quarzitic schist (Pragian)
- 55 Schönberg Formation; graphitic schist, dark grey marble (Lochkovian – Eifelian)
- 56 graphitic schist, carbonatic
- 57 dark grey calcitic and dolomitic marble
- 58 Taschen Formation; greenschist (Devonian?, Pre-Devonian)
- 59 Semriach Formation, phyllite (pre-Devonian)

- staurolite-garnet micaschist
- migmatitic micaschist
- simple pegmatite
- leucogranite
- moderate fractionated pegmatite
- spodumene pegmatite

N

1 km

Koralpe-Wölz Nappe System

Radegund Nappe

Rossegg Complex (Silurian – Carboniferous)

- 62 garnet-micaschist; amphibole-bearing

Waxenegg Nappe

Rappold Complex (Silurian – Carboniferous)

- 63 quartz mobilisate (Cretaceous?)
- 64 pegmatite, leucogranite; partly deformed (Permian)
- 65 calcitic marble, calcsilicate
- 66 amphibolite
- 67 staurolite-garnet-micaschist
- 68 micaschist, paragneiss; partly mylonitic
- 69 kyanite-bearing paragneiss ("Disthenflasergneis")
- 70 migmatitic micaschist and paragneiss; with pegmatitic patches

All visited outcrops will be in the Radegund Nappe of the Koralpe-Wölz Nappe System, as it contains the Permian pegmatite and leucogranite bodies. It is important to note that almost all of these bodies are deformed and characterized by a gneissic texture. This nappe is the lowermost tectonic element in the area and is built up by the Rappold Complex, consisting of paragneiss and micaschist with a few intercalations of amphibolite, marble and calcsilicate rock (NOWOTNY, 2007, 2008). Based on data from the same complex, but from other localities, the metasediments of the Rappold Complex were most probably deposited in a shelf and/or slope environment. From detrital zircons and Sr-isotopic data, a depositional age from the Silurian or Devonian to the Carboniferous can be inferred (PUHR et al., 2009; FRANK et al., 2019). Based on the occurrence of two garnet generations a polyphase metamorphic history is indicated (Fig. 7a). The first metamorphic imprint is Permian in age and proofed by Sm-Nd garnet and U-Pb monazite ages of about 275–255 Ma (GAIDIES et al., 2006; HAUZENBERGER et al., 2008). It reached up to upper amphibolite facies conditions with partial anatexis. The generated melts crystallized as pegmatitic patches, simple pegmatite, leucogranite, moderate fractionated pegmatite and spodumene pegmatite in different levels. A Sm-Nd garnet age of an moderate fractionated pegmatite from the locality Schöckelbartl (Stop 3) is 260 ± 3 Ma (GOTTHARDT, 2015), which perfectly fits to other Sm-Nd garnet and U-Th-Pb monazite ages from other pegmatite occurrences within the Rappold Complex (SCHUSTER et al., 2001; RÖGGLA, 2007). The Alpine overprint reached about 600° C and 0.1 GPa (RÖGGLA, 2007) and caused deformation of variable intensity (Fig. 7b).

Within the Rappold Complex of the St. Radegund area, certain associations of metasediments and pegmatite types show a distinct distribution (NOWOTNY, 2008). In the southeast, anatectic micaschist and paragneiss with stromatic to subordinate nebulitic texture is typical (Stop 1a). The metapelites are medium-grained, biotite-rich and often contain eye-catching muscovite flakes up to 5 mm in size. In thin sections, a mineral assemblage with alkali-feldspar + plagioclase + biotite + muscovite + garnet ± kyanite is visible (NOWOTNY, 2007). Garnet porphyroblasts are characterized by Permian cores with few relatively large inclusions of biotite, quartz and plagioclase often with a roundish shape. In contrast, the Eoalpine rims are more inclusion-rich (Fig. 7c). Sometimes the rims consist of several idiomorphic subgrains with a similar orientation, causing a rough and irregular shape of the porphyroblast. Kyanite forms aggregates composed of tiny crystals, often embedded in fine-grained muscovite (Fig. 7d) (NOWOTNY, 2007). These aggregates developed from Permian andalusite and/or sillimanite, which was transformed to kyanite during the Eoalpine overprint (SCHUSTER et al., 2004). Therein, pegmatitic patches and pegmatite(-gneiss) bodies composed of feldspar, quartz, minor muscovite and extremely scarce garnet and tourmaline appear.

Towards the overlying units in the west and north and towards high structural levels, respectively, the grain size of the matrix in the metapelites is decreasing and the large mica flakes and pegmatitic patches disappear. Instead, the pegmatite bodies get thicker even though they are strongly deformed and boudinaged (Stop 1b, 1c). Partly, they are very coarse-grained with up to 20 cm large alkali feldspar clasts (Fig. 7e). In the Raabklamm gorge, a body with a largely homogeneous medium-grained texture and a thickness of more than 100 m is present, which is referred to as leucogranite in here (Stop 1d).

In the uppermost part, staurolite-bearing garnet-micaschist with a fine-grained matrix composed of biotite + muscovite + quartz ± plagioclase is characteristic (Fig. 7f). Both staurolite and garnet show a dark grey colour due to inclusions of graphitic pigment and they may reach up to more than 1 cm in diameter. The textures can best be observed in the walls of the castle ruin Ehrenfels (Stop 2), because of the nicely weathered surfaces. Based on

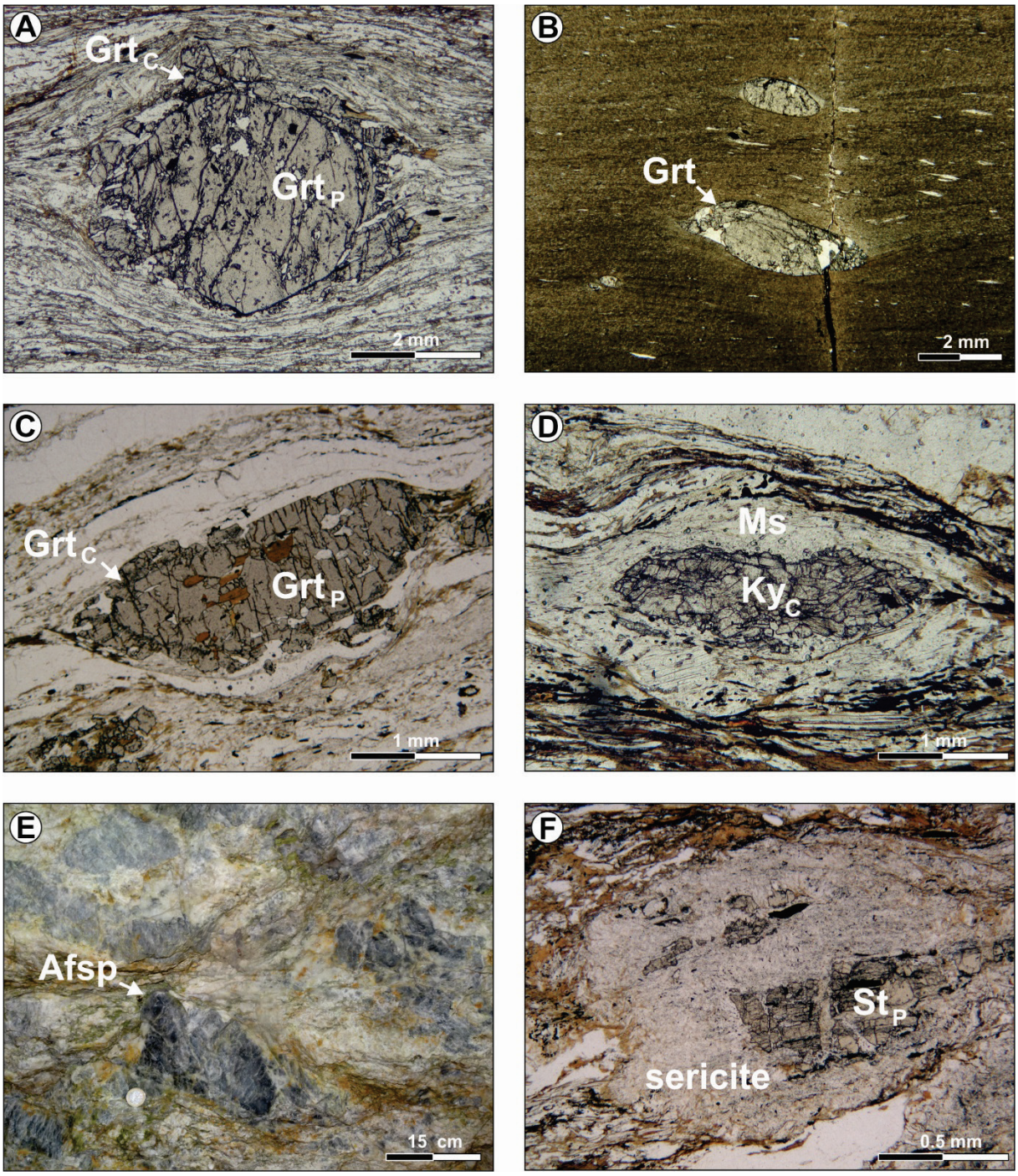

Fig. 7: *Lithologies of the Rappold Complex from the Radegund Nappe. A) Microphotograph of a micaschist with polyphase garnet with Permian core and Eoalpine (Cretaceous) rim (sample RO4-14). B) Microphotograph of an ultramylonitic micaschist (sample RA-4). C) Microphotograph of a mylonitisized migmatic micaschist with polyphase garnet. Within the garnet core larger inclusions of biotite and plagioclase are present (sample NO26-05). D) Microphotograph of a migmatic micaschist with a Cretaceous kyanite aggregate formed from Permian andalusite and/or sillimanite. Kyanite is partly replaced by muscovite (sample RK30). E) Moderate fractionated pegmatite with deformed alkali feldspar phenocrysts up to 25 cm in diameter. F) Staurolite-garnet-micaschist with Permian staurolite embedded in Cretaceous sericite (sample NO21-05). All microphotographs were taken with parallel polarizers. Abbreviations: Grt = garnet, Ms = muscovite, Ky = kyanite, Afsp = alkali feldspar, St = staurolite, P = Permian, C = Cretaceous.*

textural observations the staurolites formed contemporaneously with the Permian cores of the garnets. As in the structural lower parts of the Rappold Complex, the garnet cores are relatively poor in inclusions, but in this position, they contain mostly quartz and ilmenite instead of biotite and plagioclase. The Eoalpine garnets are again rich in inclusions mostly represented by graphitic pigment and quartz. Their chemical zoning is characterized by a significantly lower grossular component with respect to the rims (see detailed descriptions e.g. in EISENBERG & HAUZENBERGER, 2001; GAIDIES et al., 2006; RÖGGLA, 2007). In this uppermost part, additionally spodumene and beryl occur in the pegmatite gneiss bodies. One spodumene pegmatite (Stop 4) is known from the locality Schöcklkreuz at Rabnitzberg hill (ANGEL, 1933; KOLLER et al., 1983; GASSNER, 2001; GOTTHARDT, 2015) and a second one (Stop 5) forms an outcrop with a length of 12 m and a minimal thickness of 4 m in a valley close to the village of Garrach (AHRER, 2014). 20 km further to the east, the Rappold Complex appears near to the village Anger. There, a spodumene pegmatite has been described by ESTERLUS (1983).

Spodumene is up to several centimeters in size and shows a white colour. Due to alterations, it may be slightly greenish or brownish (AHRER, 2014). The Li_2O content is in the range of 6.56–7.83 wt% (KOLLER et al., 1983). Beryl is very scarce and inconspicuous with a badly preserved idiomorphic shape and a pale greyish or bluish colour. Exceptionally, it reaches several centimeters in length.

Chemical compositions (e.g. Li content, K/Rb ratio) of cm-sized magmatic muscovites from simple pegmatite, leucogranite, moderate fractionated pegmatite and spodumene pegmatite reveal a regional zoning (Fig. 8). Most peculiar is the upward decrease of the K/Rb ratio in the rock column, which reflects the upward migration of melts that get continuously fractionated. It also indicates an upright position of the Rappold Complex with respect to the Permian configuration.

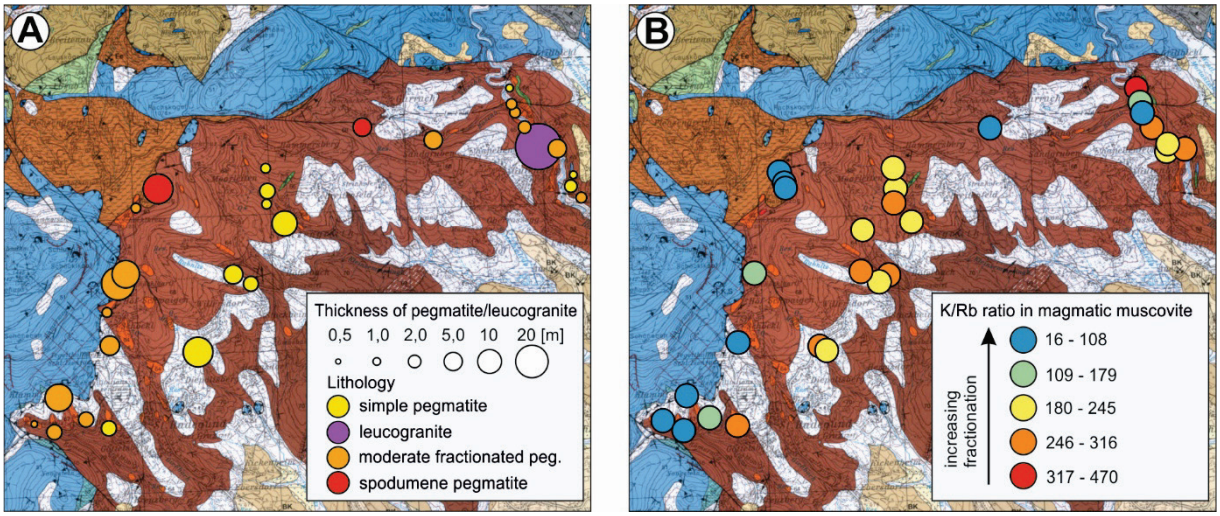

Fig. 8: *Cutout from a database dealing with Permian pegmatite and leucogranite in the Eastern Alps. Visible is the area around the village St. Radegund (Styria/Austria) based on maps in the scale 1:50,000 from the Geological Survey of Austria (legend see Fig. 6). In A) pegmatite bodies and their thickness are displayed. In B) the K/Rb ratio from magmatic muscovites is plotted. The data indicate a clear fractionation trend with decreasing ratios towards the top of the Rappold Complex. This implies an upward increasing fractionation trend and therefore an upright position of the Rappold Complex with respect to the Permian configuration.*

In a detailed study on pegmatite samples from the structurally uppermost part of the Rappold Complex, KOLLER et al. (1983) investigated the Li, Be and F content of 67 whole rock samples and corresponding muscovite and feldspar. In the whole rocks, they found less than 50 ppm Li in almost all samples, but in a few spodumene-bearing samples it reaches up to 8,500 ppm. The Li content is correlated to the modal amount of muscovite, as the latter contains a few hundred ppm Li in most cases. In the whole rocks Be is typically less than 5 ppm but reaches up to 159 ppm in the highest fractionated samples, whereas in the muscovites it is 1.0–9.7 ppm. F is 100–260 ppm in the whole rocks and 565–2,310 ppm in muscovites. The F content in the whole rock is much less than in the upper continental crust (557 ppm, RUDNICK & GAO, 2003) or granites (~850 ppm, TUREKIAN & WEDEPOHL, 1961). This fits to the observation that topaz has not been found in any of the Permian pegmatite bodies.

4. Description of stops

Stop 1 Raabklamm gorge: walk from migmatite to leucogranite (Fig. 9)

Locality: ÖK50 sheet 164 Graz, outcrops along the hiking path in the Raabklamm gorge.

Parking: At the parking site beside the former restaurant Jägerwirt.

Stop 1a: Migmatic micaschist

(WGS 84, 15°34'35.4"E / 47°12'18.9"N)

The outcrops of migmatic micaschist are situated directly along the road beside the former restaurant Jägerwirt. The rocks in the structurally lower part in the southeast have a dominant stromatic to subordinate nebulitic texture, but the differentiation of paleosome and melanosome in this outcrop is difficult. It is mostly layered metatexite formed by 0.5 cm thick in-situ leucosome and 0.5 cm thick melanosome. The leucosome contains quartz + alkali feldspar ± plagioclase ± muscovite ± small garnet and the melanosome is composed of biotite + garnet + muscovite + plagioclase ± quartz.

A few meters further to the northwest along the road, coarse-grained micaschist with partly migmatic texture and up to 0.5 cm large muscovite flakes, aligned within the foliation planes, occurs. Patchy migmatite formed by lensoidal leucosome elongated parallel to the schistosity and graphite-rich paleosome layers are common. The Eoalpine schistosity of the micaschist dips moderately towards SW (217/38).

On the way to Stop 1b several outcrops with smaller bodies of simple pegmatite-(gneiss) occur on both sides of the path.

Stop 1b: Simple pegmatite

(WGS 84, 15°34'15.1"E / 47°12'50.3"N)

The simple pegmatite body in this outcrop is > 5 m wide and embedded in fine-grained, brownish to greyish coloured micaschist. The Eoalpine schistosity penetrates partly the pegmatite forming a gneissic texture. The main mineral assemblage is quartz + alkali feldspar ± plagioclase ± muscovite ± garnet (< 0.3 cm). Alkali feldspar can be identified by its

greyish-blue colour, whereas plagioclase is white. Rarely some black tourmaline with a maximum size of 0.5 cm occurs. The Eoalpine schistosity dips shallowly towards SSW (202/15).

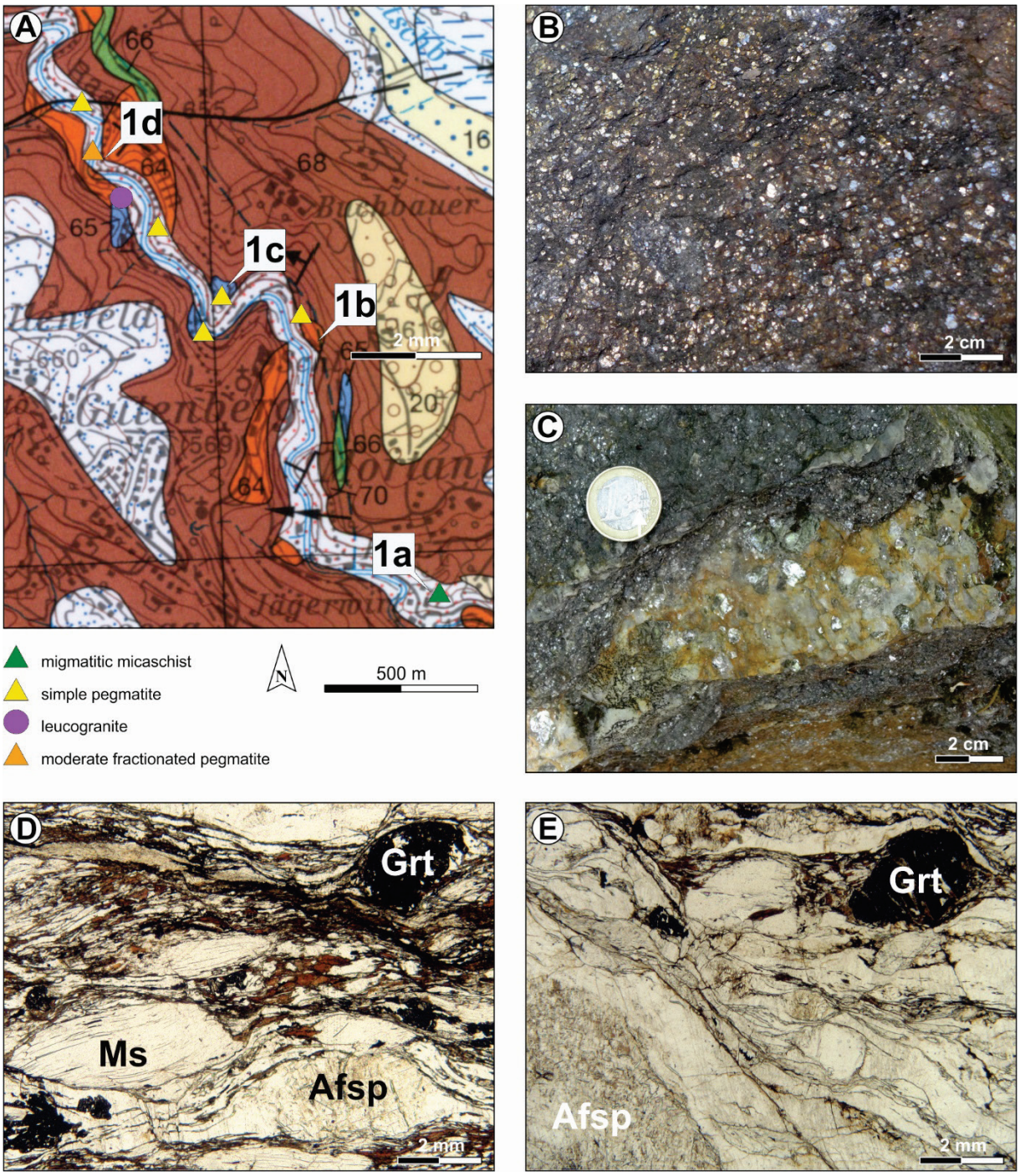

Fig. 9: *Outcrops of Stop 1 and lithologies of Stop 1a. A) Geological map (FLÜGEL et al., 2011) showing a part of the Raabklamm gorge with the four outcrops described in the text. Additionally, the analysed samples from migmatic micaschist, simple pegmatite, leucogranite and moderate fractionated pegmatite are plotted. Legend for lithologies see Figure 6. B) Migmatic micaschist from Stop 1a with large muscovite flakes aligned to the schistosity. C) Pegmatitic patch within migmatic micaschist in Stop 1a. D) Microphotograph of a migmatic micaschist with large muscovite flakes, garnet and alkali feldspar (sample 17R16; parallel polarizers, Stop 1a). E) Microphotograph of a migmatic micaschist with the transition from the paragneiss to a pegmatitic patch with a large alkali feldspar (sample 17R16; parallel polarizers; Stop 1a). Abbreviations: Grt = garnet, Ms = muscovite, Afsp = alkali feldspar.*

Stop 1c: Simple pegmatite

(WGS 84, 15°34'3.7"E / 47°12'52.5"N

Fig. 10: *Lithologies of Stop 1c. A) Outcrop of layered marble and calcsilicate rock with pegmatite boudins marked by the white dotted line (size of hammer is 0.5 m). B) Microphotograph of a calcsilicate rock composed of calcite + quartz + plagioclase + phlogopite + (clino)zoisite + titanite ± tremolite + opaque ore minerals (sample 17R12, parallel polarizers). Abbreviations: Pl = plagioclase, Zoi = zoisite, Cc = calcite, Phl = phlogopite.*

In this outcrop, a simple pegmatite situated within folded marble, calcsilicate rock and micaschist can be observed (Fig. 10). The contact of the pegmatite with marble has an intricate geometry showing a “bubbly” boudinage like structure. The pegmatite boudins have a thickness of about 0.5 m and a length that is only a little bit larger. The boudins may have formed during the emplacement of the pegmatitic melt within the marble/calcsilicate rock, or during Eoalpine deformation. The pegmatite dike in contact to the micaschist has a maximum thickness of 2 m. The main mineral assemblage of the pegmatite is quartz + alkali feldspar ± plagioclase ± muscovite (< 2 cm) ± tourmaline (< 3 cm). Marble and calcsilicate rock have a white to greyish colour and they show diffuse transitions. While the marble is more coarse-grained and mostly consists of calcite, the calcsilicate rock is fine-grained, inhomogeneous and composed of calcite + quartz + plagioclase + phlogopite + (clino)zoisite + titanite ± tremolite + opaque ore minerals. The micaschist is dark brown, fine to medium-grained and relatively rich in biotite. The Eoalpine schistosity dips moderately towards N (350/32), the fold axis is approximately E–W oriented.

Stop 1d: Leucogranite-gneiss

(WGS 84, 15°33'50.5"E / 47°13'3.1"N)

The leucogranite-gneiss forms an about 100 m thick body, which is disclosed along both sides of the gorge, forming up to 20 m high cliffs. Mostly, it shows a homogeneous fine to medium-grained texture and a mineral assemblage of quartz + alkali feldspar ± plagioclase ± muscovite and additionally small amounts of garnet and tourmaline as ferromagnesian minerals. Locally, inhomogeneous parts with pegmatitic texture occur. Mostly, it shows a penetrative Eoalpine schistosity.

Stop 2 Castle ruin Ehrenfels: staurolite-garnet-micaschist (Fig. 11)

Locality: ÖK50 sheet 164 Graz, outcrops along the hiking path to and around the castle ruin.

Parking: Beside the main road underneath the castle ruin Ehrenfels.

(WGS 84, 15°28'28.322"E / 47°10'45.834"N)

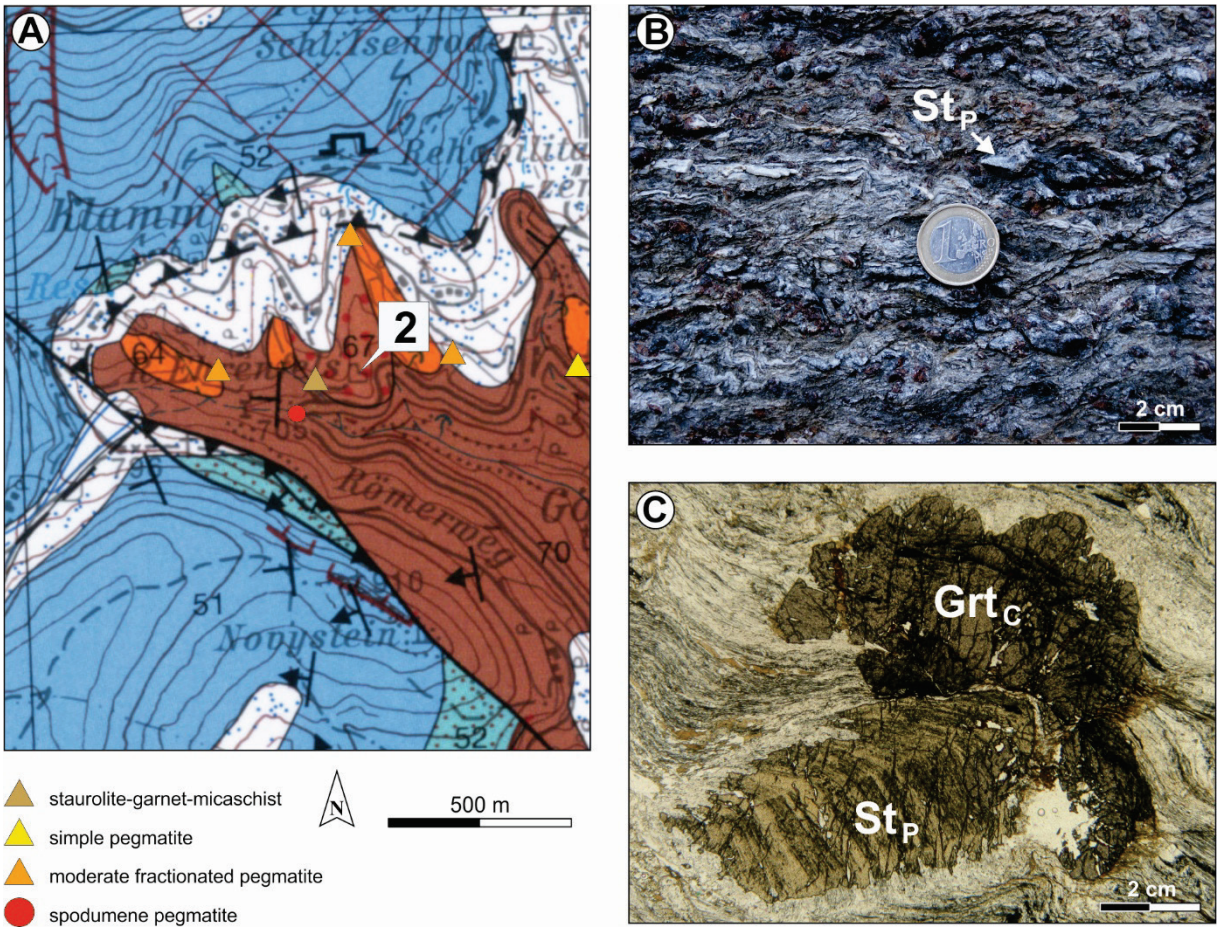

Fig. 11: *Location and lithologies of Stop 2. A) Geological map (FLÜGEL et al., 2011) showing the area around the castle ruin Ehrenfels. Additionally, the analysed samples from simple pegmatite, moderate fractionated pegmatite, spodumene pegmatite and staurolite-garnet-micaschist are plotted. Legend for lithologies see Figure 6. B) Dark gray staurolite-garnet-micaschist in the wall of ruin Ehrenfels. The Permian garnet cores show a reddish color, whereas the staurolite (St) is black. C) Microphotograph of a staurolite-garnet-micaschist (sample 05R04, parallel polarizers). Abbreviations: Grt = garnet, St = staurolite, P = Permian, C = Cretaceous.*

In the tiny outcrops along the path, dark greyish staurolite-garnet-micaschist with a fine-grained matrix is present. Staurolite-rich garnet-micaschist is best exposed in the walls of the castle ruin Ehrenfels, because of the nicely weathered surfaces (Fig. 11B). These rocks were digged in the immediate surrounding. Both, staurolite and garnet are up to more than 1 cm in diameter and show a dark grey colour due to inclusions of graphitic pigment. Garnet is polyphase with a sometimes reddish Permian core and an irregular shaped Eoalpine rim. Based on textural relations, the staurolite formed together with the garnet cores. It shows nice graphite inclusion trails and is partly or fully transformed into sericite (Fig. 11C).

Stop 3: Restaurant Schöcklbartl: moderately fractionated pegmatite (Fig. 12)

Outcrop: ÖK50 sheet 164 Graz, along a hiking path and at the road “Schöcklstraße” beside the restaurant “Schöcklbartl”.

Parking: At parking ground directly beside the road “Schöcklstraße” in front of the outcrop.

(WGS 84, 15°29'14.3"E / 47°11'57.2"N)

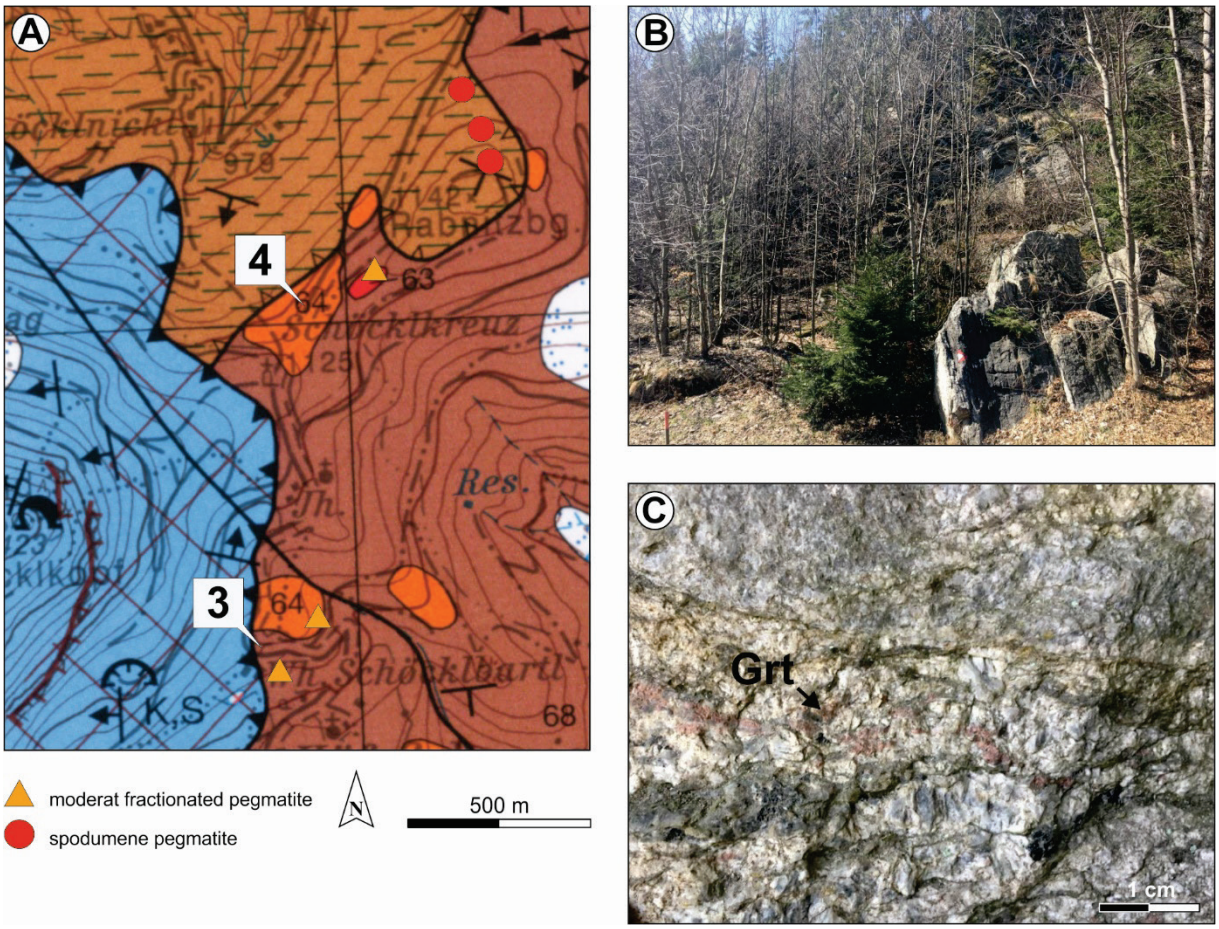

Fig. 12: *Locations of Stop 3 and 4 and lithologies of Stop 3. A) Geological map (FLÜGEL et al., 2011) showing the area around Schöcklkreuz. Additionally, the analysed samples from moderate fractionated pegmatite and spodumene pegmatite are plotted. Legend for lithologies see Figure 6. B) Outcrop of moderate fractionated pegmatite within the forest. From this pegmatite body a Sm-Nd garnet age yields 260 ± 3 Ma (GOTTHARDT, 2015). C) Garnet-rich layer within the outcrop of Figure 12B.*

Along the hiking path, several meters high outcrops (Fig. 12B) of a moderate fractionated pegmatite dike are present in the forest. The rocks show the usual magmatic assemblage quartz + alkali feldspar + plagioclase ± muscovite, but layers with garnet (Fig. 12C) and/or tourmaline also occur. The rocks exhibit a strong Eoalpine foliation.

Stop 4: Schöcklkreuz: beryl-bearing pegmatite (Fig. 12)

Outcrop: ÖK50 sheet 164 Graz, boulders beside the road “Schöcklstraße” northwards of the “Schöcklkreuz”.

Parking: Directly beside the road “Schöcklstraße”.

(WGS 84, 15°29'18.1"E / 47°12'30.0"N

On both sides of the road and around the summit of Rabnitzberg (Altitude 1142 m), several pegmatite boulders with < 2 m in size and a main mineral assemblage of quartz + alkali feldspar ± plagioclase ± muscovite are scattered in the forest. Rarely, beryl with a tabular shape occurs as up to 25 mm large crystals with a badly preserved idiomorphic shape and a milky white to pale blue colour. Some bolders of spodumene pegmatite can be found along the hiking path from Schöcklkreuz to restaurant Schöcklnickl (Walter Postl, pers. com.).

Stop 5: Garrach: spodumene pegmatite (Fig. 13)

Locality: ÖK50 sheet 164 Graz, outcrop in the forest near the path “Schneidebertl Weg”

Parking: Beside the fire brigade at the beginning of the path “Schneidebertl Weg” in Garrach

(WGS 84, 15°32'1.0"E / 47°13'2.6"N)

From the parking ground, a forest road follows the northern side of a smooth valley towards the west. After about 700 m small outcrops are visible on the southern side of the valley (Fig. 13B). They mostly consist of a spodumene pegmatite body, which can be traced for about 10 m with a maximal width of 4 m. The contact to the surrounding micaschist and paragneiss is not visible. After AHRER (2014), five zones can be distinguished within the pegmatite body: (1) The outer part is fine-grained, showing a penetrative Eoalpine schistosity. The main mineral assemblage consists of quartz + alkali feldspar + plagioclase ± garnet ± spodumene. (2) In a medium to coarse-grained zone the feldspar content is less than in zone (1), whereas the quartz, muscovite (< 0.5 cm) and spodumene (< 1 cm) contents raise. (3) A coarse-grained zone composed of quartz + alkali feldspar + plagioclase ± garnet with frequent spodumene crystals up to 3 cm in size (Fig. 13C, D, E). (4) A medium to coarse-grained zone rich in muscovite (< 3 cm) with additional quartz + alkali feldspar + plagioclase ± garnet. (5) The core zone contains up to decimeter sized albite crystals with medium to coarse-grained quartz and spodumene. Tourmaline occurs as accessory in some zones as < 4 cm long crystals. Around the spodumene pegmatite body, greyish-brown, fine-grained micaschist occurs. Biotite and muscovite form the foliation planes. In some parts, idiomorphic garnet (< 0.2 cm) occurs. The Eoalpine schistosity dips moderatly towards W (278/29).

Acknowledgements

The authors thank Walter Postl and Kurt Krenn (Karl-Franzens University of Graz) for providing additional information and photos from the field. Christine Hörfarter is acknowledged for her logistic assistance during the excursion.

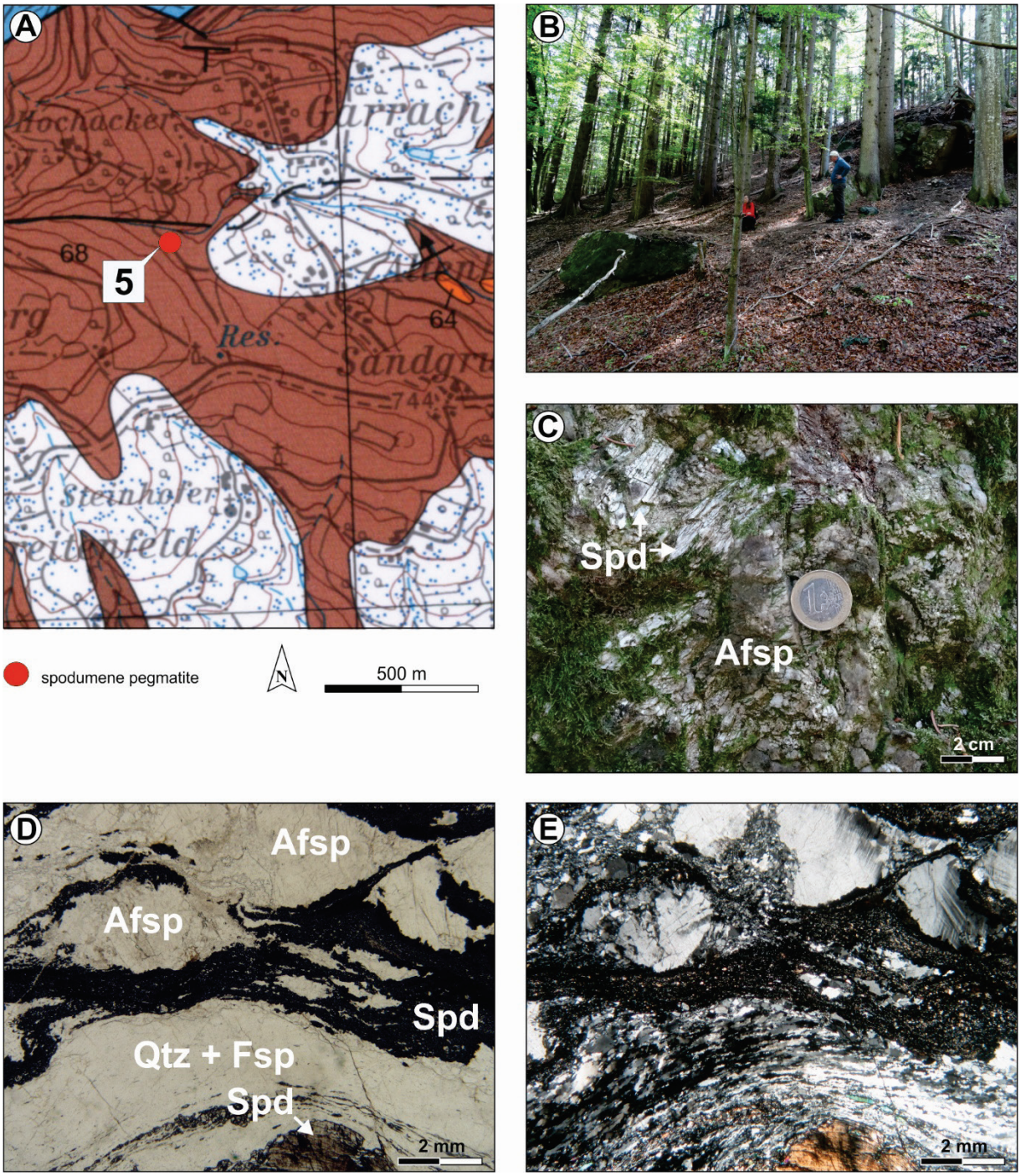

Fig. 13: *Location and lithologies of Stop 5. A) Geological map (FLÜGEL et al., 2011) showing the area around Garrach with the investigated spodumene pegmatite. Legend for lithologies see Figure 6. B) Spodumene pegmatite outcrop described by AHRER (2014) at the southern side of the valley. C) White spodumene crystals within a matrix with alkali feldspar, plagioclase and quartz. D + E) Microphotograph of mylonitized spodumene pegmatite (sample 17R11, parallel and crossed polarizers). Abbreviations: Spd = spodumene, Afsp = alkali feldspar, Fsp = alkali feldspar and plagioclase, Qtz = quartz.*

References

AHRER, S. (2014): Geowissenschaftliche und aufbereitungstechnische Untersuchungen an ausgewählten Pegmatiten und deren Nb-Ta-Vererzungen in den Ostalpen, Steiermark, Österreich. – Unpublished Master Thesis, Montanuniversität Leoben, 105 pp., Leoben.

ANGEL, F. (1933) Spodumen und Beryll aus den Pegmatiten von St. Radegund bei Graz. – Zeitschrift für Kristallographie, Mineralogie und Petrographie, **43**/6, 441–446, Leipzig.

CASSINIS, G., PEROTTI, C.R. & RONCHI, A. (2012): Permian continental basins in the Southern Alps (Italy) and peri-mediterranean correlations. – International Journal of Earth Sciences, **101**/1**,** 129–157, Berlin–Heidelberg.

ČERNÝ, P. & BURT, D.M. (1984): Paragenesis, crystallochemical characteristics, and geochemical evolution of micas in granite pegmatites. – In: BAILEY, S.W. (Ed.): Micas. – Reviews in Mineralogy, **13**, 257–297, Washington, D.C.

ČERNÝ, P. & ERCIT, T.S. (2005): The classification of granitic pegmatites revisited. – The Canadian Mineralogist, **43**/6, 2005–2026, Quebec.

DAVIS, H.J. & VON BLANKENBURG, F. (1995): Slab breakoff: A model of lithosphere detachment and its test in the magmatism and deformation of collisional orogens. – Earth and Planetary Science Letters, **129**, 85–102, Amsterdam.

DUNKL, I., GRASEMANN, B. & FRISCH, W. (1998): Thermal effects of exhumation of a metamorphic core complex on hanging wall syn-rift sediments: an example from the Rechnitz Window, Eastern Alps. – Tectonophysics, **297**, 31–50, Amsterdam.

EISENBERG, J. & HAUZENBERGER, C. (2001): Geologisch-petrologische Geländebeobachtungen des nordwestlichen Radegunder Kristallins. – Mitteilungen des naturwissenschaftlichen Vereins für Steiermark, **131**, 5–17, Graz.

ESTERLIUS, M. (1983): Kurzer Überblick über die Pegmatite im Angerkristallin der Oststeiermark. – Archiv für Lagerstättenforschung der Geologischen Bundesanstalt, **3**, 31–34, Wien.

FLÜGEL, H.W., NOWOTNY, A. & GROSS, M. (2011): Geologische Karte der Republik Österreich 1:50,000, Blatt 164 Graz. – Geologische Bundesanstalt, Wien.

FRANK, N., KURZ, W., HE, D., SCHUSTER, R., DONG, Y. & HAUZENBERGER, C. (2019): Detrital U/Pb zircon age distribution in metasedimentary units of the Eastern Alps. – EGU General Assembly 2019, Geophysical Research Abstracts, **21**, EGU2019-17014-1, Katlenburg-Lindau.

FROITZHEIM, N., PLAŠIENKA, D. & SCHUSTER, R. (2008): Alpine tectonics of the Alps and Western Carpathians. – In: MCCANN, T. (Ed.): The Geology of Central Europe. Volume 2: Mesozoic and Cenozoic, Geological Society of London, 1141–1232, London.

FROITZHEIM, N., SCHMID, S.M. & FREY, M. (1996): Mesozoic paleoegeography and the timing of eclogitefacies metamorphism in the Alps: A working hypothesis. – Eclogae Geologicae Helvetiae, **89**/1, 81–110, Basel.

FÜGENSCHUH, B., SEWARD, D. & MANCKTELOW, N. (1997): Exhumation in a convergent orogen: the western Tauern window. – Terra Nova, **9**, 213–217, Oxford.

GAIDIES, F., ABART, R., DECAPITANI, C., SCHUSTER, R., CONNOLLY, J.A.D. & REUSSER, E. (2006): Characterisation of polymetamorphism in the Austroalpine basement east of the Tauern Window using garnet isopleth thermobarometry. – Journal of metamorphic Geology, **24**, 451–475, Oxford.

GASSNER, M. (2001): Geochemische und petrologische Untersuchungen an ausgewählten steirischen Pegmatiten (Koralpe, Stubalpe, Kristallin von St. Radegund, Anger-Kristallin). – Unpublished Master Thesis, Montanuniversität Leoben, 176 pp., Leoben.

GENSER, J. & NEUBAUER, F. (1989): Low angle normal faults at the eastern margin of the Tauern window (Eastern Alps). – Mitteilungen der Österreichischen Geologischen Gesellschaft, **81**, 233–243, Wien.

GÖD, R. (1989): The spodumene deposit at "Weinebene", Koralpe, Austria. – Mineralium Deposita, **24**, 270–278, Berlin.

GOTTHARDT, C. (2015): Pegmatitgenese des Radegunder Kristallins, des Millstätter Kristallins und der Kreuzeckgruppe. – Unpublished Master Thesis, Technische Universität Graz, 156 pp., Graz.

HABLER, G. & THÖNI, M. (2001): Preservation of Permo-Triassic low-pressure assemblages in the Cretaceous high-pressure metamorphic Saualpe crystalline basement (Eastern Alps, Austria). – Journal of Metamorphic Geology, **19**, 679–697, Oxford.

HAUZENBERGER, C., ROEGGLA, M., SCHUSTER, R. & NOWOTNY, A. (2008): New petrological results from the "Anger" and "Radegund Crystalline", two polymetamorphic Austroalpine basement occurrences east of the Tauern window (Alps, Austria/Europe). – Abstract Volume "2nd Workshop and Summer School on Architecture of Collisional Orogens: Eastern Alps versus China Central Orogenic Belt", September 5–15, 2008, Department of Geology, Northwest University Xian (China), 20–22, Xian.

HOINKES, G., KOLLER, F., RANTITSCH, G., DACHS, E., HÖCK, V., NEUBAUER, F. & SCHUSTER, R. (1999): Alpine metamorphism of the Eastern Alps. – Schweizerische Mineralogische und Petrographische Mitteilungen, **79**, 155–181, Basel.

ILICKOVIC, T., SCHUSTER, R., MALI, H., ONUK, P. & HORSCHINEGG, M. (2017): Genesis of spodumene pegmatites in the Austroalpine unit (Eastern Alps): isotopic and geochemical investigations. – Abstracts and proceedings of the Geological Society of Norway (8th International Symposion on Granitic Pegmatites, Kristiansand, 14.–19.06.2017), **2/2017**, 54–57, Oslo.

JANÁK, M., FROITZHEIM, N., YOSHIDA, K., SASINKOVÁ, V., NOSKO, M., KOBAYASHI, T., HIRAJIMA, T. & VRABEC, M. (2015): Diamond in metasedimentary crustal rocks from Pohorje, Eastern Alps: a window to deep continental subduction. – Journal of Metamorphic Geology, **33**, 495–512, Oxford.

KNOLL, T., SCHUSTER, R., MALI, H., ONUK, P., HUET, B., HORSCHINEGG, M., ERTL, A. & GISTER, G. (2018): Spodumene pegmatites and related leucogranites from the Austroalpine Unit (Eastern Alps): field relations, petrology, geochemistry and geochronology. – The Canadian Mineralogist, **56**, 489–528, Quebec. http://dx.doi.org/10.3749/canmin.1700092

KOLLER, F., GÖTZINGER, M.A., NEUMAYER, R. & NIEDERMAYR, G. (1983): Beiträge zur Mineralogie und Geochemie der Pegmatite des St. Radegunder Kristallins und der Gleinalpe. – Archiv für Lagerstättenforschung der Geologischen Bundesanstalt, **3**, 47–65, Wien.

KUNZ, B.E., MANZOTTI, P., VON NIEDERHÄUSERN, B., ENGI, M., DARLING, J.R., GIUNTOLI, F. & LANARI, P. (2018): Permian high-temperature metamorphism in the Western Alps (NW Italy). – International Journal of Earth Sciences, **107**/1, 203–229, Berlin–Heidelberg.

KURZ, W. & FRITZ, H. (2003): Tectonometamorphic evolution of the Austroalpine Nappe Complex in the central Eastern Alps – consequences for the Eo-Alpine evolution of the Eastern Alps. – International Geology Review, **45**, 100–127, Columbia.

LUTH, S.W. & WILLINGSHOFER, E. (2008): Mapping of the post-collisional cooling history of the Eastern Alps. – Swiss Journal of Geoscience Supplements, **101**, 207–223, Heidelberg.

MALI, H. (2004): Die Spodumenpegmatite von Brettstein und Pusterwald (Wölzer Tauern, Steiermark, Österreich). – Joannea-Mineralogie, **2**, 5–53, Graz.

MALI, H., SCHUSTER, R., KNOLL, T. & HUET, B. (2019): Zoning of pegmatite fields as a key for unraveling the internal structure of basement nappes: examples from the Eastern Alps (Austria). – EGU General Assembly 2019, Geophysical Research Abstracts, **21**, EGU2019-14565, Katlenburg-Lindau.

NEUBAUER, F., GENSER, J. & HANDLER, R. (2000): The Eastern Alps: Result of a two-stage collision process. – Mitteilungen der Österreichischen Geologischen Gesellschaft, **92**, 117–134, Wien.

NOWOTNY, A. (2007): Bericht 2006 über geologische Aufnahmen auf Blatt 164 Graz. – Jahrbuch der Geologischen Bundesanstalt, **147**/3–4, 664–665, Wien.

NOWOTNY, A. (2008): Bericht 2007 über geologische Aufnahmen auf Blatt 164 Graz. – Jahrbuch der Geologischen Bundesanstalt, **148**/2, 266–26, Wien.

PUHR, B., SCHUSTER, R., HOINKES, G. & MOSHAMMER, B. (2009): $^{87}Sr/^{86}Sr$ isotope study of marbles. – Abstract Volume, 9th Workshop on Alpine Geological Studies (Cogne/Italy), 16.–18. September 2009, 83, Cogne.

QUICK, J.E., SINIGOI, S. & MAYER, A. (1995): Emplacement of mantle peridotite in lower continental crust, Ivrea-Verbano zone, northwest Italy. – Geology, **23**, 739–742, Washington, D.C.

RATSCHBACHER, L., FRISCH, W., NEUBAUER, F., SCHMID, S.M. & NEUGEBAUER, J. (1989): Extension in compressional orogenic belts: The Eastern Alps. – Geology, **17**, 404–407, Washington, D.C.

RÖGGLA, M. (2007): Petrographie und Petrologie des Anger Kristallins, Steiermark. – Unpublished Master Thesis, Naturwissenschaftliche Fakultät der Karl-Franzens-Universität-Graz, 168 pp, Graz.

RUDNICK, R.L. & GAO, S. (2003) Composition of the Continental Crust. – In: RUDNICK, R.L. (Ed.): The Crust, 1–64, Oxford (Elsevier-Pergamon).

SANDER, B. (1921): Zur Geologie der Zentralalpen. – Jahrbuch der Geologischen Staatsanstalt, **71**/3–4, 174–224, Wien.

SCHARF, A., HANDY, M.R., FAVARO, S., SCHMID, S.M. & BERTRAND, A. (2013): Modes of orogen-parallel stretching and extensional exhumation in response to microplate indentation and roll-back subduction (Tauern Window, Eastern Alps). – International Journal of Earth Science (Geologische Rundschau), **102**/6, 1627–1654, Heidelberg.

SCHMID, S., SCHARF, A., HANDY, M. & ROSENBERG, C. (2013): The Tauern Window (Eastern Alps, Austria): a new tectonic map, with cross-sections and a tectonometamorphic synthesis. – Swiss Journal of Geosciences, **106**, 1–32, Basel.

SCHUSTER, R. & STÜWE, K. (2008): The Permian Metamorphic Event in the Alps. – Geology, **36**/8, 303–306, Washington, D.C. http://dx.doi.org/10.1130/G24703A.1

SCHUSTER, R., SCHARBERT, S., ABART, R. & FRANK, W. (2001): Permo-Triassic extension and related HT/LP metamorphism in the Austroalpine – Southalpine realm. – Mitteilungen der Gesellschaft der Geologie- und Bergbaustudenten in Österreich, **44**, 111–141, Wien.

SCHUSTER, R., KOLLER, F., HOECK, V., HOINKES, G. & BOUSQUET, R. (2004): Explanatory notes to the map: Metamorphic structure of the Alps – Metamorphic evolution of the Eastern Alps. – Mitteilungen der Österreichischen Mineralogischen Gesellschaft, **149**, 175–199, Wien.

SCHUSTER, R., ILICKOVIC, T., MALI, H., HUET, B. & SCHEDL, A. (2017): Permian pegmatites and spodumene pegmatites in the Alps: Formation during regional scale high temperature/low pressure metamorphism. – Abstracts and proceedings of the Geological Society of Norway (8th International Symposion on Granitic Pegmatites, Kristiansand, 14.–19.06.2017), **2/2017**, 122–125, Oslo.

SCHUSTER, R., HUET, B., KNOLL, T. & PAULICK, H. (2019): Anatectic origin of albite-spodumene pegmatites: a geochemical model. – EGU General Assembly 2019, Geophysical Research Abstracts, **21**, EGU2019–7277, Katlenburg-Lindau.

STÖCKERT, B. (1987): Das Uttenheimer Pegmatitfeld (Ostalpines Altkristallin, Südtirol) Genese und alpine Überprägung. – Erlanger geologische Abhandlungen, **114**, 83–106, Erlangen.

STÜWE, K. & SCHUSTER, R. (2010): Initiation of subduction in the Alps: Continent or ocean? – Geology, **38**, 175–178, Boulder.

THÖNI, M. (1999): A review of geochronological data from the Eastern Alps. – Schweizerische Mineralogische und Petrographische Mitteilungen, **79**, 209-230, Basel.

THÖNI, M. (2006): Dating eclogite-facies metamorphism in the Eastern Alps – approaches, results, interpretations: a review. – Mineralogy and Petrology, **88**/1/2, 123–148, Wien.

THÖNI, M. & MILLER, C. (2000): Permo-Triassic pegmatites in the eo-Alpine eclogite-facies Koralpe complex, Austria: age and magma source constraints from mineral chemical, Rb-Sr and Sm-Nd isotopic data. – Schweizerische Mineralogische und Petrographische Mitteilungen, **80**, 169–186, Zürich. http://dx.doi.org/10.5169/seals-60959

THÖNI, M., MILLER, C., ZANETTI, A., HABLER, G. & GOESSLER, W. (2008): Sm-Nd isotope systematics of high-REE accessory minerals and major phases: ID-TIMS, LA-ICP-MS and EPMA data constrain multiple Permian-Triassic pegmatite emplacement in the Koralpe, Eastern Alps. – Chemical Geology, **254**, 216–237, Amsterdam. http://dx.doi.org/10.1016/j.chemgeo.2008.03.008

TUREKIAN, K.K. & WEDEPOHL, K.H. (1961): Distribution of the elements in some major units of the earth's crust. – Geological Society of America Bulletin, **72**, 175–182, Boulder.

ZOBODAT - www.zobodat.at

Zoologisch-Botanische Datenbank/Zoological-Botanical Database

Digitale Literatur/Digital Literature

Zeitschrift/Journal: Berichte der Geologischen Bundesanstalt

Jahr/Year: 2019

Band/Volume: 134

Autor(en)/Author(s): Schuster Ralf, Knoll Tanja, Mali Heinrich, Huet Benjamin, Griesmeier Gerit E. U.

Artikel/Article: Field trip guide: A profile from migmatites to spodumene pegmatites (Styria, Austria) 1-29